Chapter 20

Quantitative Analysis of Membrane Potentials

Manus W. Ward

Abstract

The changes that occur in electrochemical gradients across biological membranes provide us with invaluable information on physiological responses, pathophysiological processes and drug actions/toxicity. This chapter aims to provide researchers with sufficient information to carry out a quantitative assessment of mitochondrial energetics at a single-cell level thereby providing output on changes in the mitochondrial membrane potential ($\Delta\psi_m$) through the utilization of potentiometric fluorescent probes (TMRM, TMRE, Rhodamine 123). As these cationic probes behave in a Nernstian fashion, changes at the plasma membrane potential ($\Delta\psi_p$) need also to be accounted for in order to validate the responses obtained with $\Delta\psi_m$-sensitive fluorescent probes. To this end techniques that utilize $\Delta\psi_p$-sensitive anionic fluorescent probes to monitor changes in the plasma membrane potential will also be discussed. In many biological systems multiple changes occur at both a $\Delta\psi_m$ and $\Delta\psi_p$ level that often makes the interpretation of the cationic fluorescent responses much more difficult. This problem has driven the development of computational modelling techniques that utilize the redistribution properties of the cationic and anionic fluorescent probes within the cell to provide output on changes in $\Delta\psi_m$ and $\Delta\psi_p$.

Key words: Plasma, mitochondrial, membrane potentials, fluorescence microscopy, confocal fluorescence, TMRM, computational modelling.

1. Introduction

The desire to accurately monitor changes in mitochondrial membrane potential ($\Delta\psi_m$) at a single-cell level has increased dramatically as mounting evidence implicates mitochondria in many roles in both the physiology and pathology of many cell types (1, 2). Indeed, much of my research has focused on the characterization of mitochondrial function during the glutamate-induced neuronal injury associated with ischemic, traumatic, and

D.B. Papkovsky (ed.), *Live Cell Imaging*, Methods in Molecular Biology 591,
DOI 10.1007/978-1-60761-404-3_20,

seizure-induced brain injury (3). Glutamate receptor overactivation is known to result in an excessive Ca^{2+} uptake leading to a rapid loss of mitochondrial bioenergetics and necrosis (4–10), a delayed apoptotic neuronal injury with a collapse of mitochondrial bioenergetics hours after the initial excitation (10–14) and neurons with a hyperpolarized $\Delta\psi_m$ that are tolerant to the stimulus (15, 16). In this injury paradigm it is also evident that rapid changes occur at the plasma membrane potential ($\Delta\psi_p$) during excitation with Ca^{2+} and Na^+ loading of the neurons that is followed by a recovery of $\Delta\psi_p$ when the glutamate stimulus is removed (16). Therefore, a specific need has been established that requires the accurate determination of changes in mitochondrial function (monitoring $\Delta\psi_m$) in situ relative to changes in the electrochemical gradient across the plasma membrane (monitoring $\Delta\psi_p$) at a single-cell level.

Fluorescent membrane-permeant cationic probes such as tetramethylrhodamine methyl and ethyl esters (TMRM, TMRE) and Rhodamine-123 have become some of the most frequently used probes for the analysis of $\Delta\psi_m$ in intact cells due to their minimal photo-toxicity, low photo-bleaching, and the ability to use them in either a quenched (aggregated probe) or non-quenched (no aggregation) mode (17, 18). Previously we have successfully utilized TMRM to monitor changes in $\Delta\psi_m$ in cerebellar granule neurons (10, 16). During these studies we also established that TMRM whole-cell fluorescence is highly sensitive to changes in $\Delta\psi_p$ (10, 18, 19). Indeed, this sensitivity of cationic fluorescent probes to changes in both $\Delta\psi_m$ and $\Delta\psi_p$ have often resulted in a misinterpretation of the fluorescent responses obtained, with changes in $\Delta\psi_m$ frequently overestimated (7, 8, 11, 18, 20–23). This anomaly has in turn driven the development of computational models that utilize the Nernstian behaviour of the cationic fluorescent probes to provide quantitative output on $\Delta\psi_m$ and $\Delta\psi_p$ from the fluorescent traces obtained (10, 16, 18, 24, 25).

Here, I outline microscopy techniques and modelling systems developed for the quantitative analysis of both $\Delta\psi_m$ and $\Delta\psi_p$ at a single-cell level using both anionic and cationic fluorescent probes. Through this series of protocols and control experiments, I aim to provide sufficient information to allow even the most novice researcher to acquire quantitative output on changes in $\Delta\psi_m$ and $\Delta\psi_p$ within any cellular system.

2. Materials

2.1. Chemicals

Poly-L-lysine, poly-D-lysine, collagen IV, soybean trypsin inhibitor, trypsin, bovine serum albumin (BSA), penicillin/

streptomycin, trypsin/EDTA solution, d-glucose, L-glutamine, nerve growth factor (NGF), *N*-methyl-D-aspartic acid (NMDA), kainic acid, glycine, tunicamycin, thapsigargin, epoxomicin, H_2O_2, menadione, carbonyl cyanide *p*-(trifluoromethoxy) phenylhydrazone (FCCP), phosphate buffer saline (PBS) tablets, NaCl, KCl, KH_2PO_4, $NaHCO_3$, Na_2SO_4, $MgCl_2$, NaOH (all from Sigma); $CaCl_2$ (Fluka), L-glutamic acid monosodium salt (Fluka), HEPES (Fluka), bortezomib (LCLabs). Distilled water (Barnstead, Milli-Q).

2.2. Media

RPMI 1640 (Lonza), MEM (Gibco/Invitrogen), horse serum (Gibco/Invitrogen), fetal bovine serum (FBS) (Sigma).

2.3. Tissue

Wistar rat pups, 7 days old (Harlan; in-house breeding), PC-12 cells (ATCC).

2.4. Instruments

Coverslips 13 mm, #1 thickness (VWR International), Willco dishes (Willco BV, the Netherlands), Haemocytometer (Hawksley, UK), Microlance 23G needles (Becton Dickinson), pH meter (Thermo Electro Corporation), perfusion chamber (Warner Instruments).

2.5. Software

MATLAB® software (Mathworks, UK). *ImageJ* free online image analysis software http://rsb.info.nih.gov/ij/features.html. *MetaMorph* Software (Molecular Devices, Berkshire, UK). *CellTrack* free online cell tracking software http://db.cse.ohio-state.edu/CellTrack.

2.6. Experimental Buffer for Microscopy Experiments

120 mM NaCl, 3.5 mM KCl, 0.4 mM KH_2PO_4, 20 mM HEPES, 5 mM $NaHCO_3$, 1.2 mM Na_2SO_4, 1.2 mM $CaCl_2$, 1.2 mM $MgCl_2$ and 5 mM glucose, pH 7.4, with NaOH (*see* **Note 1**).

2.7. Plating Cells onto Glass for Microscopy

Below are some examples of the culturing conditions required for the plating of neurons/cells on glass surface in order to carry out real-time analysis of $\Delta\psi_m$ and $\Delta\psi_p$ with fluorescence or confocal microscopy. Choice of glass coverslips or glass dishes used is dictated by the type of perfusion/cell chamber you have.

2.7.1. Plating Primary Cerebellar Granule Neurons onto Glass

1. All work carried out on animals must have ethical approval and a valid government licence prior to commencing.
2. Pre-coat glass coverslips and glass Willco dishes with poly-L-lysine or poly-D-lysine at a concentration of 5 μg/mL for at least 2 h. Then wash three times with autoclaved/filtered distilled water and leave to dry prior to the plating of the neurons (*see* **Note 2**).
3. Dissect cerebella from 7-day-old Wistar rats of both sexes and pool in ice-cold preparation buffer (500 mg glucose,

600 mg BSA, one tablet of PBS and make up to 200 mL of distilled water). Place the tissue in 0.25 mg/mL trypsin and incubate at 37°C for 20 min, with trypsinization terminated by the addition of 0.05 mg/mL soybean trypsin inhibitor.

4. Triturate the neurons in order to break up any remaining clumps of cells and resuspended in 20 mL of supplemented culture medium: 450 mL MEM, 50 mL FBS, 100 U/mL penicillin and 100 μg/mL streptomycin, 3 g d-glucose, 700 mg KCl 150 mg glutamine.
5. Place 100 μL of the cell suspension on a haemocytometer and count the cells. Live cells appear as phase bright spheres; dead cells are dark and of an irregular shape.
6. Dilute the cell suspension to a final concentration of 1×10^6 cells/mL and plate in the density required: 1 mL for Willco dishes (1×10^6 cells), 200 μL for 13-mm coverslips (2×10^5 cells).
7. Add extra media 1 h after plating (10).

2.7.2. Preparation and Plating of PC12 Cells

1. To differentiate PC12 cells, the cells are gently washed with sterile PBS and incubated for 2 min at 37°C with 0.25% trypsin/2 mM EDTA solution.
2. The PC12 cells are then resuspended in supplemented culture: RPMI 1640 (425 mL), 2 mM L-glutamine, 10% (50 mL) horse serum, 5% (25 mL) fetal bovine serum, 100 U/mL penicillin and 100 μg/mL streptomycin) and passed 6–8 times through the 23G needle to break down any clumps.
3. The cells are then counted using a haemocytometer and diluted in the supplemented culture media and seeded at the density required (Willco dish, 1 mL, 1×10^4 cells, 13 mm glass coverslips, 200 μL, 5×10^2 cells) on glass pre-coated with collagen IV (2 μg/mL) (26).
4. Plate cells to allow for 50–70% confluency on the day of experimentation.
5. The cells are allowed to settle and stick to the collagen coated glass for 8 h prior to switching on to differentiating media (RPMI 1640 (495 mL), 1% horse serum (5 mL), 100 U/mL penicillin, 100 μg/mL streptomycin and 100 ng/mL NGF) (27).

2.7.3. Preparation and Plating of Most Other Cell Lines

1. Cultured cells are washed twice with sterile PBS and incubated for 5 min at 37°C with 0.25% trypsin/2 mM EDTA solution.
2. The cells are then resuspended in the required supplemented culture media (RPMI 1640 (450 mL), 2 mM L-glutamine,

10% (50 mL) fetal bovine serum, 100 U/mL penicillin and 100 μg/mL streptomycin) with rigorous pipetting that is sufficient to break up any remaining clumps of cells.

3. The cells are then counted using a haemocytometer and diluted in the supplemented culture media and seeded to allow for 50–70% confluency (Willco dish, 1 mL, 1×10^4 cells, 13 mm glass coverslips, 200 μL, 5×10^3 cells) on the day of experimentation.
4. For most cell lines glass surfaces do not needed to be pretreated.
5. Extra media should be added 1 h after plating.

2.8. Fluorescent Probes

1. TMRE (Invitrogen) and TMRM (Invitrogen) are made up in DMSO at a concentration of 1 mM, dispensed into 50 μL and stored at –20°C.
2. Rhodamine 123 (Invitrogen) is made up in DMSO at a concentration of 10 mM, dispensed into 50 μL and stored at –20°C.
3. $DiSBAC_2$ (3) (Invitrogen) is made up in DMSO to a stock concentration of 10 mM, dispensed into 50-μL aliquots and frozen.
4. A single vial of "Membrane Potential Assay Kit" (Molecular Devices) containing the plasma membrane potential indicator (PMPI) is reconstituted in 1 mL of distilled water, and dispensed into 50-μL aliquots, and frozen (PMPI stock).

3. Methods

3.1. Examples of Image Acquisition

Fine details are dependent on the requirements of the user needs and the equipment available.

3.1.1. Confocal Fluorescence Microscopy

Carl Zeiss (Jena, Germany) 510, 5-live, 710 confocal microscopes. When using 40× and 60× oil-immersion objectives, the pinhole should be between 1.0 and 1.6 Airy units to allow for an optical slice of 1 μm. TMRM is excited at 543 nm with an HeNe laser at 2/3% of total power output and the emission collected above 560 nm with a 560 nm longpass filter. This will allow the user to resolve individual mitochondria. A larger optical slice will significantly increase fluorescence; however, individual mitochondria will not be readily resolved.

3.1.2. Wide-Field Fluorescent Microscopy

Fluorescence is observed using an Axiovert 200 M inverted microscope equipped with a 40× numerical aperture 1.3 oil-immersion objective (Carl Zeiss, Jena, Germany), polychroic

mirror, and filter wheels in the excitation and emission light path containing the appropriate filter sets (TMRM, excitation 530 ± 25 nm, emission 592.5 ± 22.5 nm; dichroic mirrors for TMRM; Semrock (Rochester, NY)). Images are recorded using a back-illuminated, cooled electron multiplying CCD camera Andor Ixon BV 887-DCS (Andor Technologies, Belfast, Northern Ireland), and the imaging setup is controlled by MetaMorph 7.1 software (Molecular Devices Ltd., Wokingham, UK).

3.2. Determination of $\Delta\psi_m$ in Living Cells

TMRM and TMRE are preferred membrane potential sensors for the quantitative assessment of $\Delta\psi_m$ in living cells. They pass through the plasma membrane better than the related Rhodamine 123 and accumulate in mitochondria (17). The transmembrane distribution of these probes is directly related to the membrane potential, thereby allowing for the accurate determination of $\Delta\psi_m$. This section describes in brief a number of techniques that are commonly used to measure $\Delta\psi_m$ and $\Delta\psi_p$; however, most of it focuses on the utilization of TMRM to provide a quantitative assessment of $\Delta\psi_m$ at a single-cell level over time.

3.2.1. Measuring Changes in $\Delta\psi_m$ with TMRE

1. Make a 1 in 10 dilution (10 μL of stock TMRE added to 90 μL of experimental buffer) of your 1 mM stock solution of TMRE in experimental buffer.
2. From the 100 μM diluted solution add 1 μL to every 1 mL of experimental buffer to give a final concentration of 100 nM TMRE.
3. Incubate cells for 15 min at 37°C, then mount the glass coverslips/dishes in the perfusion/cell chamber in experimental buffer containing 100 nM TMRE.
4. Allow at least 20 min for the temperature of all components of the imaging setup to come to a steady state.
5. Measure TMRE fluorescence using wide-field or confocal fluorescence microscopy, with optimal excitation at 540 nm and emission collected above 560 nm.
6. Ensure that TMRE is equilibrated within the cytosol and mitochondria by monitoring the TMRE fluorescence for 10–15 min and that the whole-cell fluorescence remains stable (*see* **Note 3**).
7. When the fluorescence is stable the desired stimulation (*see* **Note 4**) is applied and the fluorescence monitored.

3.2.2. Measuring Changes in $\Delta\psi_m$ with Rhodamine 123

1. Make a 1 in 10 dilution (10 μL of stock Rhodamine 123 added to 90 μL of experimental buffer) of the 10 mM Rhodamine 123 stock solution.

2. From this 1 mM diluted stock add 2.6 μL to 1 mL of loading buffer to give a loading buffer with a final concentration of 2.6 μM.
3. Cells are incubated with 2.6 μM Rhodamine 123 for 15 min in experimental buffer at 37°C prior to mounting the cells in the perfusion chamber. Alternative loading paradigms with Rhodamine 123 (26 μM) may sensitize the neurons to photo-induced damage.
4. Unlike TMRM and TMRE, Rhodamine 123 TMRE is not present in the experimental buffer during the course of the experiment.
5. Following the placement of the cells on the microscope stage allow at least 20 min for the temperature of the imaging setup to come to a steady state.
6. Rhodamine 123 fluorescence is then measured with fluorescent/confocal microscopy; excitation at 485 nm and emission collected above 520 nm.
7. A baseline Rhodamine 123 fluorescence should be measured for at least 10–15 min (**Note 3**) prior to addition of any stimulation (**Note 4**) (9, 10).

3.2.3. Measuring Changes in $\Delta\psi_m$ with TMRM

1. Make a 1 in 100 dilution (10 μL of stock TMRM added to 990 μL of experimental buffer) of your stock (1 mM) TMRM solution in experimental buffer.
2. From this 10 μM solution add the desired volume to every 1 mL of experimental buffer to give a final concentration. For example, 2 μL of 10 μM TMRM added to 1 mL of experimental buffer gives a final concentration of 20 nM.
3. Typically to work in the quenched condition, use a concentration of TMRM between 50 and 200 nM (*see* **Fig. 20.1a**) and for non-quenched conditions a concentration of less than 20 nM (*see* **Fig. 20.1b**) is desirable (*see also* **Section 3.2.5**).
4. Cells on coverslips/glass dishes have the media removed and replaced with experimental buffer containing TMRM for 30 min.
5. Replace with fresh buffer containing the loading concentration of TMRM when the coverslips/glass dish are mounted in the perfusion/cell chamber and maintain at 37°C. When using a non-perfusion chamber check to make sure that evaporation is not a major issue or seal with mineral oil.
6. Give the system a further 20–30 min for all components of the imaging setup to reach a constant temperature. Small fluctuations in temperature lead to small drifts in focus and

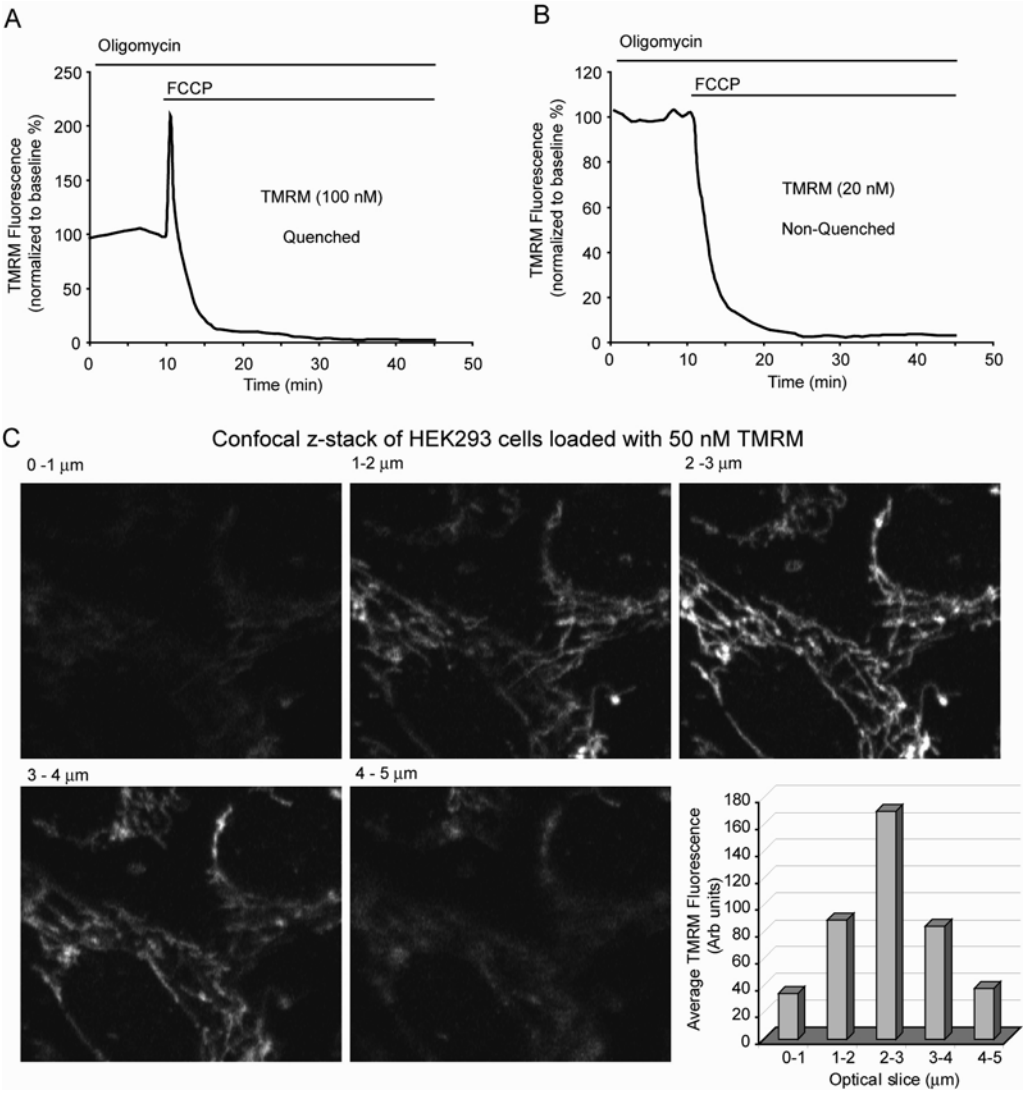

Fig. 20.1. Characterization of TMRM fluorescence in cells with high-resolution single-cell confocal microscopy. (**a, b**) Cerebellar granule neurons loaded with 100 nM TMRM (**a**) and 30 nM TMRM (**b**) were exposed to 2 μM FCCP in the presence of 2 μg/mL oligomycin and the changes in the whole-cell fluorescence monitored. (**c**) HEK293 cells were loaded with 100 nM TMRM and a high-resolution *z*-stack was acquired of the mitochondria within the cells. *Graph inset* indicates the average TMRM fluorescence within mitochondrial rich regions for each plane of the *z*-stack.

this can have major implications on the whole-cell fluorescence obtained (*see* **Fig. 20.1c, Notes 5 and 6**).

7. TMRM has a broad excitation and emission spectra with excitation of TMRM between 530 and 550 nm preferable; however, TMRM can be excited at 488 nm if required. The emission spectra for TMRM are also broad so a 560-nm longpass filter is preferred.

8. A baseline TMRM fluorescence should be measured for at least 10–15 min (**Note 3**) prior to any stimulation (*see* **Note 4**)

3.2.4. Image Analysis

The type of analysis carried out will be highly dependent on the software kinetics package associated with the imaging setup. If the associated software does not provide sufficient flexibility two other options are recommended: ***ImageJ*** (http://rsb.info.nih.gov/ij/features.html) and its Java source code are freely available and in the public domain. This software is continually updated with over 500 plug-ins available. ***MetaMorph*** Software (Molecular Devices) is a very powerful tool for image acquisition, processing, and analysis. The software package is very versatile and offers solutions for a wide range of applications. Both software packages are routinely used within our group and are highly recommended.

1. An associated kinetic package with the software will allow for the data (e.g. average intensity, integrated fluorescence and standard deviation) to be collected for each region of interest (ROI) at each time point.
2. The data is typically stored in a format that will allow it to be easily exported or opened in an Excel spreadsheet.
3. For an accurate comparison of changes in the average fluorescence intensity for multiple cells it is suggested to normalize the baseline fluorescence to 100% due to mitochondria within different cells not all being on the same *z*-plane.
4. To ensure that the traces for each region are representative of what is happening in the cell, carefully check to make sure that the cell remains within the ROI and that there are no major drifts in focus (*see* **Note 5**).
5. If cells move or change shape significantly on a regular basis, analysis should be carried out with cell tracking software (***CellTrack*** http://db.cse.ohio-state.edu/CellTrack (28) (*see* **Note 7**).

3.2.5. Determination of the Quench Limit for TMRM Within the Mitochondrial Matrix

1. The current modelling techniques for changes in $\Delta\psi_m$ are valid when working in both the quenched (1A) and non-quench (*see* **Fig. 20.1b**) modes. However, it is important to establish the concentration of TMRM in the matrix that initiates aggregation and quenching (10, 16, 24, 29).
2. Cells are equilibrated with TMRM in a concentration range from 100 to 10 nM.
3. Cells are pre-treated with oligomycin (2 μg/mL) for 10 min prior to collapsing $\Delta\psi_m$ with a protonophore (FCCP) in

order to block ATP synthase reversal and cellular ATP depletion.

4. The protonophore FCCP is added at a concentration of 2 μM, which should be sufficient to rapidly collapse $\Delta\psi_m$. If the concentration of FCCP is not sufficient then increase it to 5–10 μM. However, at these higher concentrations $\Delta\psi_p$ may also be affected (*see* **Note 8**).
5. Validation that the fluorescent changes are due to alterations of $\Delta\psi_m$ need to be carried out using the $\Delta\psi_p$-sensitive indicator $DiSBAC_2$ (3) or PMPI (**Section 3.2**).
6. If significant changes are occurring at a $\Delta\psi_p$ level, then the concentration of FCCP needs to be reduced or other channel inhibitors added (e.g. for neurons the glutamate receptor antagonists MK-801and NBQX are required (16)).

3.2.6. Estimation of the Rate Constant for TMRM Re-equilibration Across the Plasma Membrane

The relaxation constant seen in Eqs. 20.1–20.3 is due to the delay of movement of the TMRM through the plasma membrane. It is obtained in control experiments where either $\Delta\psi_p$ or $\Delta\psi_m$ are depolarized (high KCl, FCCP) and the redistribution constant for TMRM is calculated (10, 16, 24, 29). Nernstian equilibration of a generic membrane-permeant monovalent cation C^+ among the extracellular, cytoplasmic, and mitochondrial matrix phases at 37°C results in the following relationships for the concentrations of the free cations at equilibrium:

$$c^+_{[\text{matrix}]} = c^+_{[\text{cytoplasm}]} * 10^{-\Delta\Psi m/61.5} \quad (1)$$

$$c^+_{[\text{cytoplasm}]} = c^+_{[\text{medium}]} * 10^{-\Delta\Psi p/61.5} \quad (2)$$

$$c^+_{[\text{matrix}]} = c^+_{[\text{medium}]} * 10^{-(\Delta\Psi m+\Psi p)/61.5} \quad (3)$$

where $\Delta\psi_m$ and $\Delta\psi_p$ are, respectively, the plasma and mitochondrial membrane potentials (using accepted sign conventions), and the divisor 61.5 is the value (in mV) for RT/F at 37°C. Re-equilibration of the cytosolic and extracellular compartments due to changes in the potentials of $\Delta\psi_p$ and $\Delta\psi_m$ are taken into account by assuming a first order flux between the extracellular medium and the cytosol:

$$J_{[\text{cytoplasm}]} = \left(c^+_{[\text{cytoplasm,actual}]} - c^+_{[cytoplasm,equilibrium]}\right) k_{\text{kinetic}} \quad (4)$$

where $[k_{\text{kinetic}}]$ is a constant proportional to the permeability of the C^+ probe across the plasma membrane.

3.2.7. The Fraction of the Cell Volume Occupied by the Mitochondrial Matrices

Cellular TMRM fluorescence is not only highly dependent on the changes in both $\Delta\psi_m$ and $\Delta\psi_p$ but is also directly related to the total mitochondrial volume within the cell (10, 16, 24, 29).

Therefore, a stringent determination of the mitochondrial volume is required.

1. Cells are loaded with 50 nm TMRM.
2. High-resolution *z*-stacks with 1 μm optical slices and 0.2 μm steps are taken of 3–4 fields of cells (70–80 images per field).
3. Deconvolution software is used to create a three-dimensional image of the cells and the mitochondria. Individual mitochondria are counted and the volume of each estimated for at least three fields of cells.
4. The volume of the respective cells are calculated and the mitochondrial volume is then calculated as a percentage of the total cellular volume.

3.3. Protocols for Determination of $\Delta\psi_p$ in Living Cells

Patch clamping has long been considered the standard way to measure changes in $\Delta\psi_p$ in single cells; however, it can be a slow, labour-intensive process with relatively low throughput. To provide much faster methods that have applications within both research and industry a series of voltage-sensitive dyes have been devised that provide reliable fast responses to changes in $\Delta\psi_p$.

3.3.1. Measuring Changes in $\Delta\psi_p$ with $DiSBAC_2$ (3)

1. $DiSBAC_2$ (3) is a bis-barbituric acid oxonol compound that partitions into the membrane as a function of membrane potential. Hyperpolarization causes extrusion of the dye and decreased fluorescence, whereas depolarization causes enhanced fluorescence (30).
2. Make a 1 in 10 dilution (10 μL of stock $DiSBAC_2$ (3) added to 990 μL of experimental buffer) of your stock (10 mM) $DiSBAC_2$ (3) solution in experimental buffer.
3. From this 1 mM solution add 1 μL to every 1 mL of experimental buffer to give the desired working concentration.
4. Cells are incubated with experimental buffer containing 1 μM $DiBAC_2$ (3) for 30 min at 37°C. One micromolar $DiSBAC_2$ (3) is also present in the experimental buffer when cells are mounted on the microscope stage.
5. Optimal excitation of $DiSBAC_2$ (3) probe is at 543 nm with and the emission collected above 560 nm.
6. $DiSBAC_2$ (3) fluorescence is calibrated as a function of $\Delta\psi_p$ depolarization and is determined by quantifying the fluorescent enhancement obtained when $\Delta\psi_p$ is depolarized by increasing KCl concentrations.
7. A series of experiments can be performed in which step increases in K^+ concentrations are made by removing defined volumes of low-K medium and replacing this with an equal volume of high-K medium to give final K^+ concentrations from 3.5 to 75 mM (24).

3.3.2. Measuring Changes in $\Delta\psi_p$ with PMPI

1. The Molecular Devices "Membrane potential assay kit" has been utilized in a number of studies and has been termed PMPI, for "plasma membrane potential indicator" by David Nicholls (24).
2. Cell are washed with experimental buffer and then incubated with 0.5 μL/mL PMPI stock in experimental buffer (37°C) for 45 min prior to imaging. 0.5 μL/mL PMPI is also maintained in the experimental buffer during the course of the experiment.
3. PMPI is excited in single track mode with the 514 nm band of an argon laser and the emission collected above 570 nm with the laser intensity maintained at 1% to reduce phototoxicity.
4. PMPI fluorescence can be calibrated as above (**Section 3.2.1**, step 5).

3.4. Computational Modelling

Since fluorescently charged dyes such as TMRM respond to changes in both $\Delta\psi_m$ and $\Delta\psi_p$, the interpretation of changes in whole-cell fluorescence is often difficult. For this reason, mathematical models that exploit the Nernstian behaviour of TMRM have been used to create computer simulations and models that provide output on changes in $\Delta\psi_m$ and $\Delta\psi_p$ over time.

3.4.1. Variables

Certain variables are required prior to Data input for each cellular system. These can be obtained by carrying out the control experiments described above, namely, *establishing the mitochondrial volume fraction* of the cell (**Section 3.2.7**); inputting the *external TMRM probe concentration* (quenched and non-quench (**Section 3.2.3**)), the *TMRM rate constant k* (**Section 3.2.6**), the *quench limit* for TMRM (**Section 3.2.5**), the *PMPI rate constant* (**Section 3.2.2**) calculated from curve-fitting an experiment in which $\Delta\psi_p$ is rapidly depolarized by elevating external KCl concentration. The initial resting values for $\Delta\psi_m$ are in the region of –150 mV (24). The resting value for $\Delta\psi_p$ is typically between –60 and –80 mV (24).

3.4.2. Data Input to Computer Simulation

1. The computer simulation and accompanying notes are provided as supplemental material in http://www.jbc.org/cgi/content/full/M510916200/DC1 (24).
2. When the whole fluorescent traces for both the TMRM and PMPI have been obtained, open a copy of the master template in the supplemental data.
3. Enter the variables in the upper left hand corner (A).
4. Paste in a copy of the TMRM and PMPI traces into panel B.

5. Manually alter the potential profiles for $\Delta\psi_m$ and $\Delta\psi_p$ (H) in order that the simulation traces (C) can fit the raw data traces. This may require some time as multiple changes in both $\Delta\psi_m$ and $\Delta\psi_p$ may be required to obtain an optimal fit for the raw data.
6. When you are satisfied with the fitting a graphical form of the output for changes in $\Delta\psi_m$ and $\Delta\psi_p$ can be found in panel (E) and numerical values obtained in column (H).
7. When changing the external TMRM concentration in (A), significant changes will occur to the total simulated signal (T). To get good fits multiply the raw data by a factor so that the experimental trace and fitted trace can overlap in panel (D). A similar approach should also be adopted for fitting the PMPI experimental traces.

3.4.3. TOXI-SIM

The Nernstian properties of TMRM and how it responds to changes in both $\Delta\psi_m$ and $\Delta\psi_p$ allow for the mathematical analysis of the distribution of the probe to provide quantitative information on changes of both $\Delta\psi_m$ and $\Delta\psi_p$ over time (10, 16, 24, 25). Huber et al. (29), have built on the initial studies to develop an automated computational model TOXI-SIM (http://systemsbiology.rcsi.ie/tmrm/index.html) that is based on Newton-fitting algorithms implemented into MATLAB® software (Mathworks, UK).

Data Input for TOXI-SIM

1. In work carried in neurons stimulated with glutamate a number of clearly defined TMRM responses representing distinct injury paradigms (rapid necrosis, delayed (biphasic) necrosis, apoptosis and tolerance) were established (10, 16, 29).
2. For each injury model a mathematical model was created that can be opened by clicking on the appropriate header option (rapid necrosis, biphasic necrosis, apoptosis and tolerance) in TOXI-SIM main menu.
3. For each model the fitting variables (**Section 3.4.1**) are entered into the upper right hand panel on the web service.
4. Each variable is entered and a fitting range of either 10%, 100%, free fitting or no change is entered. The fitting range will depend on the range within which a certain variable may fall.
5. The experimental protocol parameters and cell specific initial values for $\Delta\psi_m$ and $\Delta\psi_p$ are entered in the lower right table.
6. Fluorescence traces for up to eight cells, normalized to an initial value of 100%, are entered either by copying them to the dedicated textbox in the left bottom or by directly accessing a locally stored Excel file via a browse facility.

7. The first column of the input data is dedicated to measurements time points (s, min, h) and the appropriate timescale is selected in the checkbox above the trace entry field.
8. The calculate options is then selected and the resultant fluorescent traces, fitted traces and output for $\Delta\psi_m$ and $\Delta\psi_p$ are rendered graphically and provided in an Excel format for each cell.
9. To achieve optimal fits for your data sets, the traces for the cells should be broken down into subsets that are similar to each of the models described and this option selected, i.e. do not try to fit traces similar to the apoptotic response with the necrotic model.

Data Base for Storage

1. TOXI-SIM is designed as a flat file based database for experimental storage and retrieval allowing for multiple users to access the same data sets.
2. By entering the "Submit experimental Model data" link on the main page, a form is automatically loaded that permits the submission of data sets for each of the four models.
3. Each data set allows for the entry of data time series for up to eight cells, modification of parameter and their fitting ranges as well as technical data from the experimental design.
4. The data set is given a unique name thus allowing for easy retrieval by multiple users.

Overall, the ability of computer models to simultaneously evaluate changes in $\Delta\psi_m$ and $\Delta\psi_p$ for multiple cells significantly enhances our understanding of cellular function and mitochondrial energetics in response to different stimuli, offering novel insights into how their cellular system respond. In addition the throughput capacity and reduced manual input provided by TOX-SIM allows for statistical analysis to be carried out on large populations of single cells and has the potential to be utilized in high-content screening and high-throughput screening platforms within research and industry thereby allowing for the rapid screening and characterization of drugs actions/toxicity.

The most accurate computational fittings and therefore the most accurate quantitative assessment off changes in $\Delta\psi_m$ and $\Delta\psi_p$ are obtained when the fluorescent response for the cationic and anionic fluorescent responses are representative of what is occurring within the cell. Therefore, it is essential that users ensure that the quality of the images obtained and the processing of the data is of the highest standard.

4. Notes

1. $MgCl_2$ is not added to the experimental buffer under conditions where an excitation of NMDA glutamate receptors is required.
2. A number of different coating techniques use mixtures of laminin, collagen, poly-L-lysine and poly-D-lysine for different types of neuronal populations. Please check which technique is most widely used as this can have a major influence on neuronal survival following plating, their development in culture, and behaviour on stimulation.
3. A baseline TMRM/TMRE/Rhodamine 123 fluorescence should be measured for at least 10–15 min prior to the stimulation of the cells to ensure that the loading of probe within the mitochondria and cells has come to a resting equilibrium.
4. Some example of stimuli routinely used are as follows: neuronal excitation; *NMDA (100 μM), kainate (300 μM), glutamate (100 μM)*. Endoplasmic reticulum stress; *tunicamycin (1 μM), thapsigargin (10 μM)*. Proteasomal stress; *epoxomicin (50 nM), bortezomib (100 nM)*. Oxidative stress; *H_2O_2 (50 μM), menadione (100 nM*).
5. Even small drifts of focus can dramatically alter the whole-cell fluorescence. In **Fig. 20.1c**, a *z*-stack containing five optical slices was taken through a HEK293. It is readily apparent that only a 1-μm shift up or down from the optimal optical (2–3 μm) slice results in a marked alteration in the whole -cell TMRM fluorescence. To reduce focus drifts, allow all components of the system to come to a steady temperature prior to beginning an experiment. Room temperature should be maintained within a 1–2°C window. Use a temperature controller for the objective if possible. Have your microscope on an air table or in a stable environment to reduce even the smallest of vibrations. If the microscope system allows, carry out small *z*-stacks (3–4 images, 3–4 μm) at each time point, thereby allowing for some minor drifts in focus. If your cells have drifted out of focus, stop the experiment, save data, refocus and start acquisitions again. A great deal of data can still be obtained from the experiment.
6. Choosing the best field of focus is often difficult. Some cells spread out and are flat (HEK293, *see* **Fig. 20.1c**), making it relatively easy to resolve individual mitochondria even with a standard fluorescent microscope. However, most cells are not flat; therefore, it is advisable to focus on a *z*-plane that

cuts through mitochondria-rich areas within the majority of cells.

7. Many cells move and change shape on a regular basis throughout the course of an experiment. This is particularly relevant when monitoring most cell lines over long periods of time. For this reason many groups are currently working on the development of cell tracking software that can segment and track individual cells, thereby providing an accurate assessment of changes in whole-cell fluorescence over time. Free tracking software is now available online (***CellTrack*** http://db.cse.ohio-state.edu/CellTrack (28)) and this area is a major focus of development within many imaging groups with further advancements in cell tracking technology soon available.
8. In neurons, $\Delta\psi_p$ is altered following a rapid depolarization of synaptic mitochondria with the protonophore FCCP. This rapid depolarization is believed to allow for the release of glutamate from the pre-synaptic terminal into the synaptic cleft and the activation of post-synaptic NMDA receptors.

References

1. Duchen MR. (2004) Mitochondria in health and disease: perspectives on a new mitochondrial biology. Mol Aspects Med, 25, 365–451.
2. Nicholls DG. (2004) Mitochondrial dysfunction and glutamate excitotoxicity studied in primary neuronal cultures. Curr Mol Med, 4, 149–77.
3. Choi DW. (1994) Glutamate receptors and the induction of excitotoxic neuronal death. Prog Brain Res, 100, 47–51.
4. Choi DW. (1987) Ionic dependence of glutamate neurotoxicity. J Neurosci, 7, 369–79.
5. Tymianski M, Charlton MP, Carlen PL, Tator CH. (1993) Secondary Ca^{2+} overload indicates early neuronal injury which precedes staining with viability indicators. Brain Res, 607, 319–23.
6. Budd SL, Nicholls DG. (1996) Mitochondria, calcium regulation, and acute glutamate excitotoxicity in cultured cerebellar granule cells. J Neurochem, 67, 2282–91.
7. White RJ, Reynolds IJ. (1996) Mitochondrial depolarization in glutamate-stimulated neurons: an early signal specific to excitotoxin exposure. J Neurosci, 16, 5688–97.
8. Stout AK, Raphael HM, Kanterewicz BI, Klann E, Reynolds IJ. (1998) Glutamate-induced neuron death requires mitochondrial calcium uptake. Nat Neurosci, 1, 366–73.
9. Vergun O, Keelan J, Khodorov BI, Duchen MR. (1999) Glutamate-induced mitochondrial depolarisation and perturbation of calcium homeostasis in cultured rat hippocampal neurones. J Physiol, 519 Pt 2, 451–66.
10. Ward MW, Rego AC, Frenguelli BG, Nicholls DG. (2000) Mitochondrial membrane potential and glutamate excitotoxicity in cultured cerebellar granule cells. J Neurosci, 20, 7208–19.
11. Ankarcrona M, Dypbukt JM, Bonfoco E, Zhivotovsky B, Orrenius S, Lipton SA, Nicotera P. (1995) Glutamate-induced neuronal death: a succession of necrosis or apoptosis depending on mitochondrial function. Neuron, 15, 961–73.
12. Ward MW, Rehm M, Duessmann H, Kacmar S, Concannon CG, Prehn JH. (2006) Real time single cell analysis of bid cleavage and bid translocation during caspase-dependent and neuronal caspase-independent apoptosis. J Biol Chem, 281, 5837–44.
13. Budd SL, Tenneti L, Lishnak T, Lipton SA. (2000) Mitochondrial and extramitochondrial apoptotic signaling pathways in cerebrocortical neurons. Proc Natl Acad Sci USA, 97, 6161–6.
14. Luetjens CM, Bui NT, Sengpiel B, Munstermann G, Poppe M, Krohn AJ, Bauerbach E, Krieglstein J, Prehn JH. (2000) Delayed mitochondrial dysfunction in

excitotoxic neuron death: cytochrome c release and a secondary increase in superoxide production. J Neurosci, 20, 5715–23.
15. Iijima T, Mishima T, Akagawa K, Iwao Y. (2003) Mitochondrial hyperpolarization after transient oxygen-glucose deprivation and subsequent apoptosis in cultured rat hippocampal neurons. Brain Res, 993, 140–5.
16. Ward MW, Huber HJ, Weisova P, Dussmann H, Nicholls DG, Prehn JH. (2007) Mitochondrial and plasma membrane potential of cultured cerebellar neurons during glutamate-induced necrosis, apoptosis, and tolerance. J Neurosci, 27, 8238–49.
17. Ehrenberg B, Montana V, Wei MD, Wuskell JP, Loew LM. (1988) Membrane potential can be determined in individual cells from the nernstian distribution of cationic dyes. Biophys J, 53, 785–94.
18. Nicholls DG, Ward MW. (2000) Mitochondrial membrane potential and neuronal glutamate excitotoxicity: mortality and millivolts. Trends Neurosci, 23, 166–74.
19. Farkas DL, Wei MD, Febbroriello P, Carson JH, Loew LM. (1989) Simultaneous imaging of cell and mitochondrial membrane potentials. Biophys J, 56, 1053–69.
20. Khodorov B, Pinelis V, Vergun O, Storozhevykh T, Vinskaya N. (1996) Mitochondrial deenergization underlies neuronal calcium overload following a prolonged glutamate challenge. FEBS Lett, 397, 230–4.
21. Keelan J, Vergun O, Duchen MR. (1999) Excitotoxic mitochondrial depolarisation requires both calcium and nitric oxide in rat hippocampal neurons. J Physiol, 520 Pt 3, 797–813.
22. Kiedrowski L. (1998) The difference between mechanisms of kainate and glutamate excitotoxicity in vitro: osmotic lesion versus mitochondrial depolarization. Restor Neurol Neurosci, 12, 71–9.
23. Prehn JH. (1998) Mitochondrial transmembrane potential and free radical production in excitotoxic neurodegeneration. Naunyn Schmiedebergs Arch Pharmacol, 357, 316–22.
24. Nicholls DG. (2006) Simultaneous monitoring of ionophore- and inhibitor-mediated plasma and mitochondrial membrane potential changes in cultured neurons. J Biol Chem, 281, 14864–74.
25. Dussmann H, Rehm M, Kogel D, Prehn JH. (2003) Outer mitochondrial membrane permeabilization during apoptosis triggers caspase-independent mitochondrial and caspase-dependent plasma membrane potential depolarization: a single-cell analysis. J Cell Sci, 116, 525–36.
26. Tomaselli KJ, Damsky CH, Reichardt LF. (1987) Interactions of a neuronal cell line (PC12) with laminin, collagen IV, and fibronectin: identification of integrin-related glycoproteins involved in attachment and process outgrowth. J Cell Biol, 105, 2347–58.
27. Zhdanov AV, Ward MW, Prehn JH, Papkovsky DB. (2008) Dynamics of intracellular oxygen in PC12 cells upon stimulation of neurotransmission. J Biol Chem, 283, 5650–61.
28. Sacan A, Ferhatosmanoglu H, Coskun H. (2008) CellTrack: an open-source software for cell tracking and motility analysis. Bioinformatics, 24, 1647–9.
29. Huber HJ, Plchut M, Weisova P, Dussmann H, Wenus J, Rehm M, Ward MW, Prehn JH. (2009) TOXI-SIM-A simulation tool for the analysis of mitochondrial and plasma membrane potentials. J Neurosci Methods, 176, 270–5.
30. Freedman JC, Novak TS. (1989) Optical measurement of membrane potential in cells, organelles, and vesicles. Methods Enzymol, 172, 102–22.